IEEE Access
Multidisciplinary | Rapid Review | Open Access Journal

SPECIAL SECTION ON BATTERY ENERGY STORAGE AND MANAGEMENT SYSTEMS

Received January 22, 2018, accepted February 18, 2018, date of publication February 21, 2018, date of current version May 16, 2018.

Digital Object Identifier 10.1109/ACCESS.2018.2808412

A Comparison of Online Electrochemical Spectroscopy Impedance Estimation of Batteries

MINA ABEDI VARNOSFADERANI AND DANI STRICKLAND
Holywell Park, Loughborough University, Loughborough L11 3TU, U.K.

Corresponding author: Mina Abedi Varnosfaderani (m.abedi-varnosfaderani@lboro.ac.uk).

This work was supported by the EPSRC and Project Manifest under Grant EP/N032888/1.

ABSTRACT This paper compares the methods of undertaking on-line electrochemical impedance spectroscopy that have been published in the literature. This paper describes the different published methodologies and sorts these into categories. This paper looks at the theoretical analysis of the circuits and control techniques and follows up with simulation and/or experimental studies of these methods. This paper focuses on battery systems.

INDEX TERMS Batteries, impedance spectroscopy, impedance measurement.

I. INTRODUCTION

A key challenge in a battery energy storage system [1] is understanding the availability and reliability of the system from the perspective of the end customer. A key task in this process is recognising when a battery or a module within a system starts to degrade and then mitigating against this using the control system or battery management system. Battery characterisation parameters such as internal impedance, state of health (SOH) and state of charge (SOC) are useful means of representing battery conditions.

The quantity of published literature in reputable journals around Electrochemical Impedance Spectroscopy (EIS) indicates that these measurements are a valuable tool in determining the impedance and the subsequent states of the battery. EIS is a method of data measurement which looks at the electrical and electrochemical characteristics of some material or electrical components such as a battery. An EIS test is usually performed by applying a small AC excitation signal into a test piece and measuring its response using a four-wire system. The frequency response of the test piece is produced to understand how its impedance changes over the frequency domain. Traditionally EIS methods were performed on battery systems when the battery was disconnected from the system. Offline EIS equipment tends to be expensive but is known for its accuracy.

In battery systems where it is necessary to keep the battery on-line for availability purposes, it is not desirable to have to disconnect the battery for testing. Therefore, some attempts have been made to reproduce an online version. Much of this work is recent in nature (within the last three years) and has been developed independently at different research establishments.

This paper compares and classifies these different methods. Some of these techniques are not specifically related to batteries but may be adapted for measuring battery impedance and have therefore been included. Fig. 1 is an attempt at separating these different methodologies into classifications.

Fig. 1 also shows where further techniques may be developed by highlighting areas where online EIS measurements are not currently being considered. The classification starts by differentiating between offline and online measurements. An on-line method refers to a technique where the battery is still connected with a system and is able to operate independently of the measurements been undertaken.

Offline EIS measurements have been used by a number of authors over the years to undertake research into estimation of accurate battery model parameters; at different SOC or SOH [2]–[13]; at different temperatures [9], [14]–[16]; with different materials [17]–[20], and under charge/discharge cycling to look for degradation [21]–[24]. Table 1 shows a summary of the applied offline EIS testing conditions and excitation voltage and current limits for different types of batteries undertaken by these authors. These measurement methods have been in use for over twenty years [25] and are well established.

One of the challenges with online methods is to produce an excitation signal at different values of frequency with a magnitude similar to those values in Table 1 and detect the response to these signals under normal operational conditions when other voltage and currents are present.

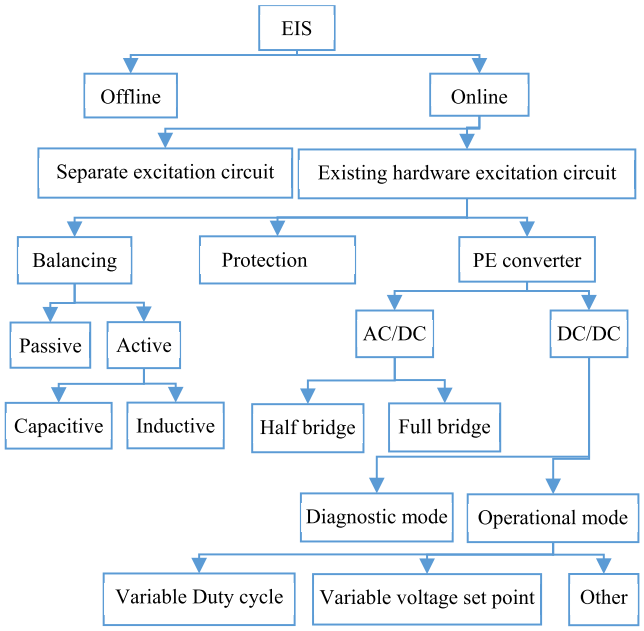

FIGURE 1. Different battery EIS methods.

TABLE 1. Offline batteries EIS testing conditions reported in literature.

Battery type	Frequency Range	Excitation Amplitude
Lithium-ion [2]–[4], [8], [10], [20]	3 MHz to 10mHz	3mV to 62.5mV 0.1A to 1A
Lead acid [5], [11], [18], [26]	10MHz-1mHz	5mV to 10mV 60mA to 0.1A
Nickel metal [12], [15], [19], [24]	10MHZ-50 µHz	-5mV to 10mV 40mA to 100mA

Figure 1 takes the online methods and splits these into those that require additional hardware to provide a separate excitation and those methods that use existing hardware to generate the EIS excitation. These include the battery balancing circuitry, the protection devices and the power electronic converter.

This work is organised around these different methods of producing the excitation signal as follows: Section II describes online topologies using separate excitation circuit, Sections III to VI looks at methods using existing hardware. Where Section III looks at the techniques using the battery balancing circuitry, Section IV looks at online methods using AC/DC power electronic converters, Section V looks at online methods using DC/DC power electronic converters and Section VI looks at using protection based circuitry. Section VII looks at other aspects of the methods and Section VIII compares these methods and concludes the paper with a discussion on the methodologies.

II. SEPARATE EXCITATION CIRCUIT

This technique generates an excitation signal, separate from the main battery system, through the use of separate bespoke circuits. Neti and Grubic [27] used a separate excitation circuit for EIS calculations on a three phase induction machine rather than a battery. In this paper, the excitation signal was reported as being generated between phase and ground using a coupling circuit over the frequency range of 10kHz to 9.5Mhz. Reference [28] used a signal processing circuit to inject an EIS excitation signal directly to a battery. The signal processing circuit converted a voltage signal generated from Labview software into a current signal and measured the voltage response to calculate the impedance of the battery. The current excitation signal is injected each time with a different frequency at frequency interval of 0.01Hz to 1kHz. Wang *et al.* [29] and Tröltzsch and Kanoun [30] used a power amplifier to generate a separate excitation signal. In this method, the impedance was calculated over the frequency ranges of 0.01Hz to 1kHz and 3mHz to 10311Hz respectively.

There has been mention of sinusoidal charging of batteries using sinusoidal ripple current (SRC) as opposed to CV and CC (constant voltage and constant current) as a means improving charging performance [31]. This is done by adding a separate AC excitation signal to the battery system. The frequency was swept from 1Hz to 1200Hz. Recent work [32] has looked at the possibility of using this to undertake EIS measurements over the frequency range of 0.1Hz to 6.31Hz. The methodology lacks detail in the published literature and although an EIS diagram is produced, it is not clear whether the method is online as the EIS plot is shown for three OCV conditions. However, there is no perceptible barrier as to why this shouldn't be made online.

References [33] and [34] employed a pseudo-random binary sequence (PRBS) current pulse perturbation to measure the impedance of the battery online. This method used a band limited pseudo-random noise signal to excite the battery current and then measure the voltage response of the battery at frequency intervals of 1Hz to 1kHz [33] and 80Hz to 2kHz [34]. This noise signal can be superimposed either as an addition to the control signal or in isolation to excite the battery. The main disadvantage of this method is the small signal to noise ratio as a result of the smaller amplitude of the measured battery voltage frequency response compared to the amplitude of the noise signal. This can be improved by using a very large input which may result in nonlinear behaviour of the system.

III. EXISTING HARDWARE – BATTERY BALANCING

This classification uses hardware in the battery balancing circuitry to inject the variable frequency excitation signal. Currently attempts have been made to introduce EIS measurement using the shunt resistor, ladder inductor, and switched capacitor battery balancing circuiting. However, there is no reason why other methods of balancing couldn't be tried also.

A. SHUNTING RESISTOR BALANCING

Koch *et al.* [35] introduces three methods of online impedance measurement. One of these uses battery balancing as a means of producing an excitation signal, to estimate the battery impedance over the specific frequency range of 10mHz to 2kHz. In battery balancing, a balancing

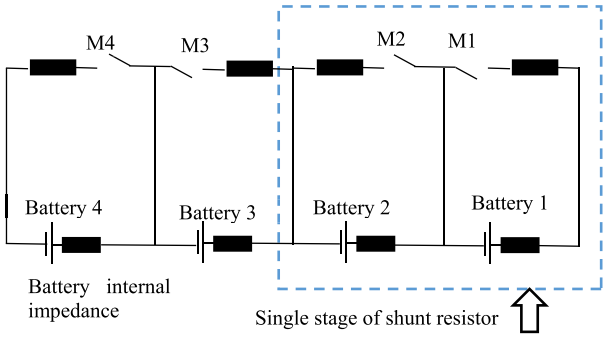

FIGURE 2. Shunt resistor balancing operation circuit.

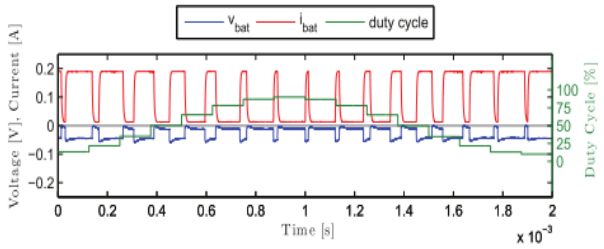

FIGURE 3. Shunt resistor time domain signal of i_{bat}, v_{bat} and corresponding duty cycle by modulating the excitation current signal [35].

resistor with a switch was used to excite the battery, as shown in Fig. 2.

This method is sensitive to the balancing current, which results in SOC changes after each measurement. This is because the balancing circuit can only discharge the battery. The battery current is excited by modulating the switches of the balancing circuit. The current and voltage of the batteries were measured using a DS1278 Delta-Sigma (ADC) from a STM32F407 Digital Signal Processor. The reproduced excited battery current and voltage are shown in Fig. 3.

B. LADDER INDUCTOR BALANCING

References [36] and [37] are work by the same authors who use an inductive based battery balancing system for online EIS measurement over frequency range of 25mHz to 7.66kHz. Two battery cells are connected to a ladder inductor battery balancing circuit using a switched-inductor bidirectional buck-boost converter as a building block of a ladder converter. The perturbation signal was generated by a digital signal synchronised in a FPGA and injected by the controller to the switches in the ladder circuit as shown in Fig. 4.

When switch M1 is on, battery 1 is connected in parallel with the converter and the converter operates for time DT_s. The converter is then connected in parallel with battery 2 to transfer the energy when switch M2 is on for a time (1-D) T_s, where D is the duty cycle that the balancing switches are operated with. The battery voltage is excited by a voltage perturbation signal induced by a controller algorithm. The excitation signal is defined as a voltage difference between

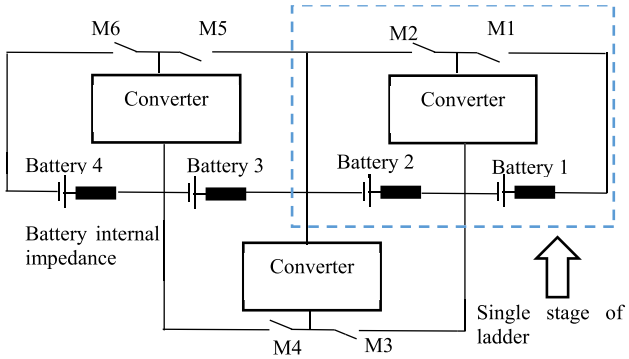

FIGURE 4. Ladder circuit balancing operation.

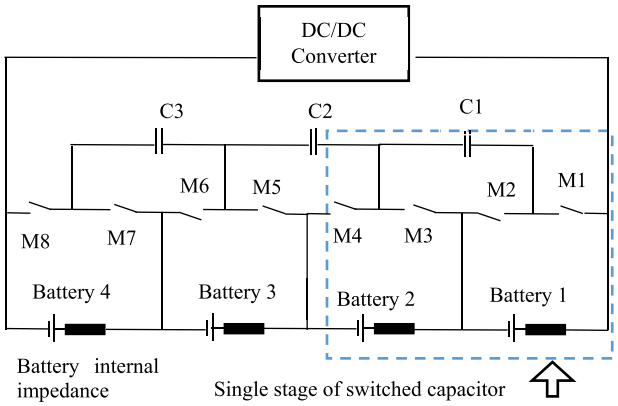

FIGURE 5. Switched capacitor battery balancing circuit.

the voltage of battery 1 and battery 2 for a single stage of balancing system. Din *et al.* [36], [37] used TI ADS7254 12-bit ADCs and ADS7254 12-bit ADCs to measure the battery current and voltage to calculate the battery impedance.

C. SWITCHED CAPACITOR BALANCING

Varnosfaderani [38] used a straightforward switched capacitor balancing system to generate the low-frequency excitation signal as a proof concept due to its popularity in literature. The schematic of 4 battery cells with a dc/dc converter and the switched capacitors balancing technique is shown in Fig. 5. The switched capacitor system is connected to the battery and it is used to inject a low-frequency signal at frequency interval of 1Hz to 2kHz.

The author uses a single stage of the switched capacitor balancing circuit. In this circuit, switches M1 – M4 were operated to produce a low-frequency excitation signal. The value of the capacitor was chosen so that the variable-frequency switching allows energy transfer between the two batteries. To avoid a short-circuit condition or current shoot-through, two pulse signals with a duty cycle of less than 0.5 were used for controlling the switches M1-M4 [39].

Author uses IL300 voltage sensor and ACS712 current sensor measurement devices linked to the controller to get an EIS measurement. The battery voltages are subject to a

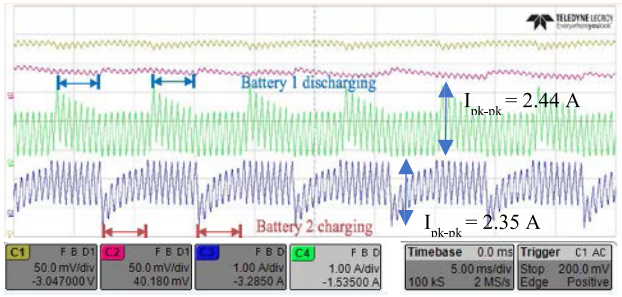

FIGURE 6. Measured 2.5Ah Li-ion battery voltage (top) and current waveforms (bottom), with an added low frequency excitation of 125Hz. Y axis --> Time (s) and X axis --> Amplitude (1A/div).

small perturbation caused by the balancing capacitor charging and discharging. The low-frequency excitation presents in the charging and discharging waveforms is shown in Fig. 6. In this method the batteries are discharged at an average constant value of 1.2A. Although this excitation is non-sinusoidal, the low frequency component of interest can be extracted using FFT.

The author reported that this method may not be useful when there is either a high voltage difference between the two batteries - because this results in a high value of capacitor current, or when the battery voltages are equalised as the low-frequency ripple is not visible in the waveforms. However, there is clearly research scope to expand these types of methods to investigate excitation with other battery balancing topologies.

IV. EXISTING HARDWARE – AC/DC POWER ELECTRONICS

These classifications use AC/DC power electronics system converter as a means of generating the excitation signal. In these examples, the system under test (typically a battery) is connected directly to the power converter. These methods can be further sub-divided into half bridge and full bridge topologies. The half bridge circuit allows battery charging through rectification, while, the full bridge circuit allows for full bi-directional functionality.

References [40], [41], and [35] are published works by the same authors, who use a half bridge AC/DC converter to inject the EIS excitation signals over frequency range of 10mHz to 5kHz to a battery. This process is uni-directional and is undertaken on battery charging only. The battery charger is connected to a number of battery cells and excites the battery cells by injecting a carrier frequency excitation signal to the converter switches. The variation of the current and voltage ripple of the battery is illustrated in Fig. 7. Koch *et al.* [40] and Koch and Jossen [41] used a MCP3903 Sigma-Delta (ADC) to and a ADS1278 Sigma-Delta ADC measure the battery current and voltage. The authors reported that the synchronisation of the battery current during the measurement is a disadvantage of the method (i.e. the battery cannot simultaneously charge and discharge) as the current needs to be measured.

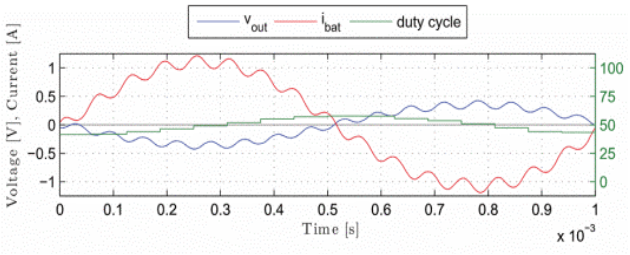

FIGURE 7. Measured current and voltage of the single cell with multisine excitation [35].

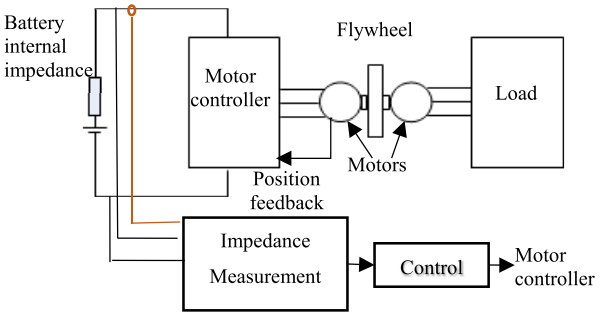

FIGURE 8. Motor inverter topology within a vehicle drivetrain.

Reference [42] measured the impedance of the battery by using a motor inverter to generate the low-frequency excitation required to look at battery impedance within vehicle drivetrain as shown in Fig. 8. The measured current and voltage of a battery cell were excited with a multisine perturbation waveform over a frequency range of 1Hz to 2kHz. In this method, a shunt resistor and a RS 363-6810 Audio Precision APX525 network were used for battery current and voltage sensing. The excitation signal comes from the main traction current of the motor. The key disadvantage of the method is that the excitation current is produced from the motor and it's not clear what impact this has on motor operation. For example, good results may be limited to the machine fundamental frequency. So, it may not be possible for the frequency to be swept across a range of as this may impact operation.

V. EXISTING HARDWARE – DC/DC POWER ELECTRONICS

This classification considers energy storage connected to a DC-DC power electronics system prior to connection through an inverter to the grid system. This section focuses on the methods and impact of measuring battery impedance through the power electronics using a straightforward boost/buck circuit. However, the methodology is applicable for more complex topologies. The method of introducing a small excitation signal through the DC/DC power electronics is primarily a function of different forms of control. These methods can be split into diagnostic mode (very similar to offline methods) and normal operational mode. The normal operational mode can also be split into different methods used to introduce a

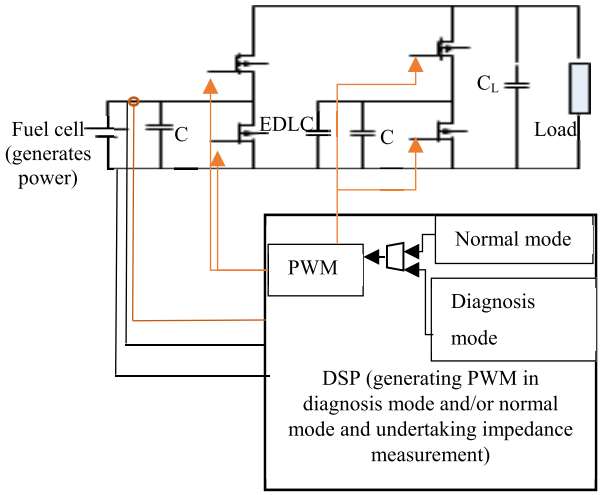

FIGURE 9. Diagnostic mode of online EIS using a DC/DC converter.

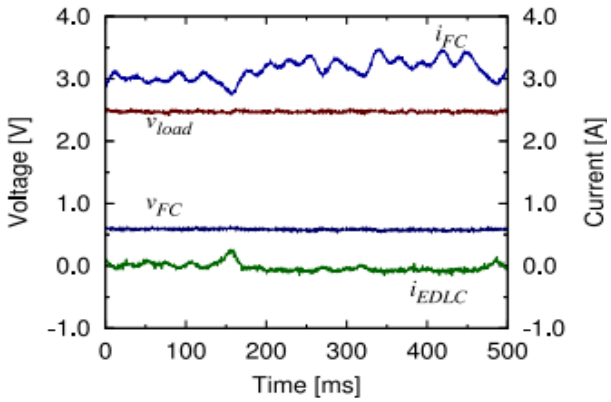

FIGURE 10. Waveforms of the load voltage, electric double layer capacitor (EDLC) current, and fuel cell voltage and current when the superimposed signal is applied [43].

low-frequency signal. These methods include using a variable voltage set point, variable duty cycle, variable switching frequency, variable starting position and adding an impulse function.

A. DIAGNOSTIC MODE

Reference [43] used a hybrid power source of a fuel cell and electric double layer capacitor (EDLC) with bidirectional dc/dc converter hardware, as shown in Fig. 9. The EDLC is used to reduce the load fluctuation of the fuel cell. The bidirectional converter is used to control the fuel cell under normal operating conditions and also to provide an AC excitation signal under a diagnostic setting when the fuel cell was not operational. The excitation signal was injected at two frequency range of 95.4mHz–36.6Hz and 12.2Hz–4.69kHz.

Fig. 10 shows the reported excited voltage and current waveform when a superimposed signal is applied to the fuel cell through the controller in diagnostic mode. The excited voltage and current were measured by built in sensors in a DSP board. The Author reported that the proposed method

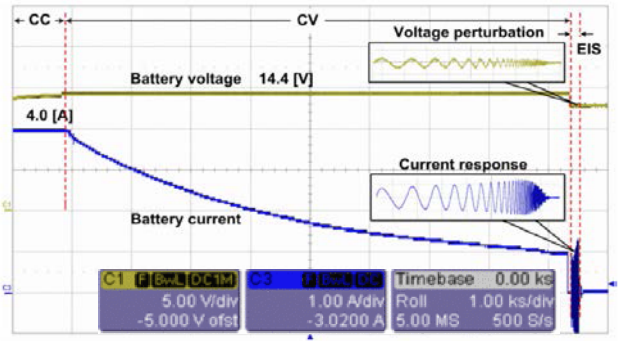

FIGURE 11. Charge & EIS operation variable voltage set point using 40Ah lead-acid battery [44]. Y axis --> Time (s) and X axis --> Amplitude (1A/div).

shows good agreement with the offline measured impedance values. However, the impedance of a fuel cell is higher than a battery and if this method were to be applied to a battery it would need to be taken off-line to undertake the diagnostics.

B. OPERATIONAL MODE – VARIABLE VOLTAGE SET POINT

Nguyen *et al.* [44] used a bidirectional converter circuit with a control system to generate a small excitation voltage signal for impedance measurement and SOH estimation. In this method the battery was charged with CC/CV battery charging method and was excited with a sinusoidal voltage perturbation signal. As shown in Fig. 11, the excitation signal is a sinusoidal voltage signal added by the voltage controller loop to excite the battery over the frequency range of 0.1Hz to 1kHz. This method was introduced for the SOH prediction of the battery, the impedance is measured only after the battery is fully charged using DSP TMS320F28335. Reference [45] uses the same method but uses a phase shift dc/dc converter to duplicate the impedance measurement. The difference between the methods is the control and bandwidth of the bi-directional converter that is used for the EIS measurement.

C. OPERATIONAL MODE – VARIABLE DUTY CYCLE

The dc/dc converter is operated such that the average duty cycle is considered constant (as if the system were operating in steady state), but the instantaneous duty cycle is varied to add a low-frequency component in order to induce a low frequency harmonic into the circuit as shown in Fig. 12 [45]–[47].

The excitation signal is injected to the converter by varying the duty cycle of the switching PWM signal. An example of the waveform obtained using this method is shown in Fig. 13 (the battery is discharged at an average constant value of 1.2A).

Reference [46] uses the same method but uses multi-sine signals to measure the impedance of the battery with multiple harmonics at the same time rather than at a single frequency point each time. Abu Qahouq and Xia [47] used the same hardware but used the control system to add a change to the output voltage set point to create a perturbation of multiple

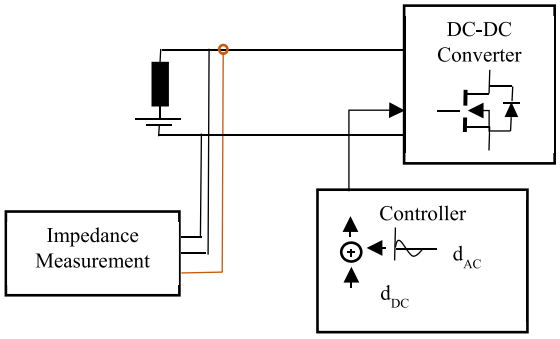

FIGURE 12. Schematic of operation of online EIS using a DC/DC converter with variable duty cycle.

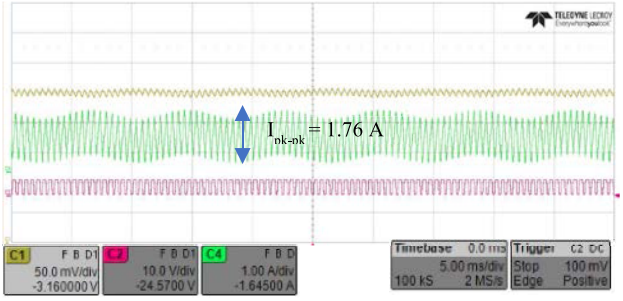

FIGURE 13. Measured 2.5Ah Li-ion battery Current (Middle) and Voltage (Top) waveforms. The battery is excited with PWM (bottom) with a variable duty cycle with a low frequency component of 125Hz. [37]. Y axis --> Time (s) and X axis --> Amplitude (1A/div).

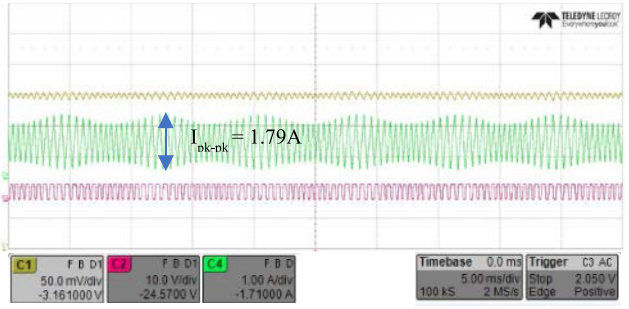

FIGURE 14. Measured 2.5Ah Li-ion battery Current (Middle) and Voltage (Top) waveforms. The battery is excited with PWM (bottom) and variable switching frequency with a low frequency component of 125Hz [37]. Y axis --> Time (s) and X axis --> Amplitude (1A/div).

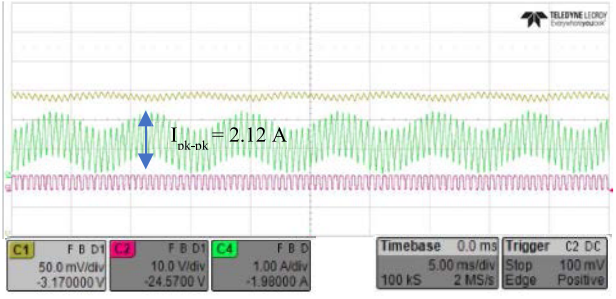

FIGURE 15. Measured 2.5Ah Li-ion battery Current (Middle) and Voltage (Top) waveforms. The battery is excited with PWM (bottom) with variable starting position with a low frequency component of 125Hz. [49]. Y axis --> Time (s) and X axis --> Amplitude (1A/div).

frequencies (200Hz to 3.8kHz) to capture more data over a shorter period of time. The current and voltage data were captured by a digital controller. The proposed method suffers from the lack accuracy as the frequency order increases. Densmore and Hanif [48] used the same method but used an AC voltage ripple excited by the modulated duty cycle of the converter at a single frequency point of 500Hz. Then the battery voltage and current response were measured and analysed using DSP TI F2833 to estimate the impedance and state of charge of the battery at that single frequency.

D. OPERATIONAL MODE – VARIABLE SWITCHING FREQUENCY

Reference [38] uses a different method of injecting low-frequency harmonics to measure the batteries impedance. In this method, the dc/dc converter is operated such that the switching frequency (as opposed to duty cycle) has the same average value but now oscillates around this value with a low frequency to induce a low frequency into the gate drive circuit. The current is excited with the induced perturbation signal to the converter gate drive. The experimental variation of the battery voltage and current waveform (discharging at 1.2A) is shown in Fig. 14. These waveforms were measured using IL300 voltage sensor and ACS712 current sensor measurement devices.

The impedance of the battery was calculated by harmonic analysis of these waveforms across different values of low-frequency (1Hz - 2kHz). The author reported that the resultant calculated impedance based on measured data using this method is not sufficiently accurate to be useful as a means of looking at on-line battery impedance. This is because the derived value of the low-frequency harmonic component is very low and this leads to a loss of accuracy.

E. OPERATIONAL MODE – VARIABLE STARTING POSITION

Varnosfaderani [38] also introduced an online method of battery impedance measurement using a pulse position modulation method. In this method of injecting a low-frequency component to the battery circuit, the current is excited with the modulated pulse control signal of the power electronic converter. The reported battery voltage and current waveform ripple variation (discharging at 1.2A) with the induced excitation signal are shown in Fig. 15.

In this method, the switching frequency is fixed as is the duty cycle, but the starting position of the "on" signal varies within the switching period. However, this starting position has been shifted to allow a sinusoidal variation about the midpoint of the switching time period. A challenge in this method, is that the "on" pulse shouldn't cross over to either of the adjacent switching periods, so the variation of position is limited by this. Another challenge of this method is that the results are also potentially subject to hardware limitations.

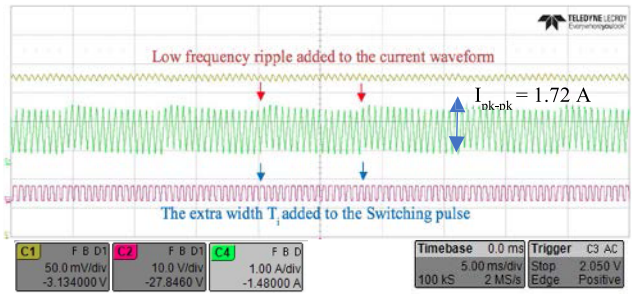

FIGURE 16. Measured 2.5Ah Li-ion battery Current (Middle) and Voltage (Top) waveforms. The battery is excited with a PWM (bottom) with an impulse function at a low frequency of 125Hz [38]. Y axis --> Time (s) and X axis --> Amplitude (1A/div).

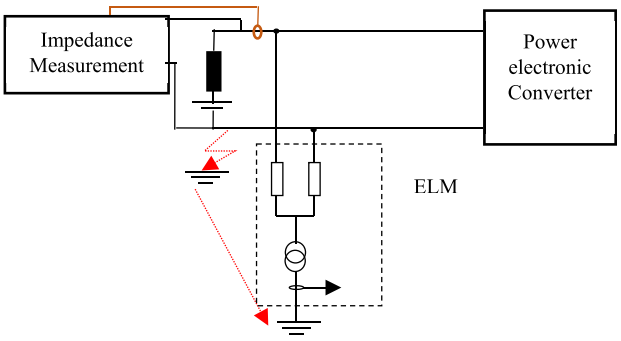

FIGURE 17. A representation of an Earth Leakage Monitoring circuit in operation [52].

F. OPERATIONAL MODE – IMPULSE FUNCTION

Reference [38] introduced an alternative method of adding a low-frequency harmonic into the gate drive circuit by adding a low-frequency impulse function. The low-frequency signal is injected to the battery current as a combination of the impulse function with the usual switching frequency pulse waveform using an OR function. In this method the author used integer values of low-frequency pulse waveforms for convenience in conjunction with an OR function. However, the author reported that the duty cycle of the low-frequency pulse should be sufficient so that when passed through an OR function with the pulse train it results in an increase in the pulse width. This is shown in Fig. 16. The battery current (discharging at 1.2A) is excited at each interval the switching pulse is added.

VI. EXISTING HARDWARE – PROTECTING CIRCUITRY

This section looks at a different method of injecting a low-frequency excitation signal by manipulating protection circuitry. At this point in time, only an Earth Leakage Monitoring (ELM) relay hardware has been investigated as a source of excitation. There are a different number of commercial earth leakage monitoring which include devices which detect and monitor both ac and dc circuits [50] and those that look only at dc systems [51]. An example of the operation of ELM device is shown in Fig. 17.

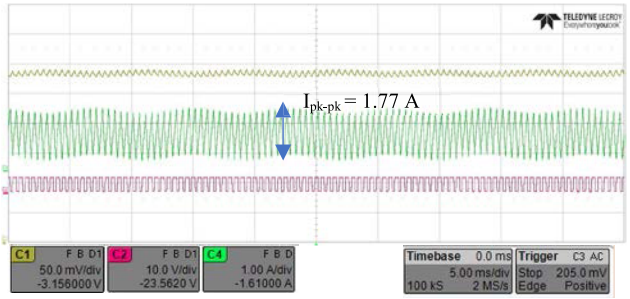

FIGURE 18. 2.5Ah Li-ion battery Current (Middle) and Voltage (Top) waveforms. The battery is excited with a fixed duty cycle PWM (bottom) and a low frequency ELM signal at 125Hz [52] Y axis --> Time (s) and X axis --> Amplitude (1A/div).

An ELM circuit typically has two sources. In [52], the AC sources were used to produce a common mode signal to detect earth faults and a differential signal across the battery to produce the excitation signal at frequency range of 1Hz to 2kHz. Fig. 18 shows the added low frequency excitation ripple to the battery (discharging at 1.2A) waveforms from the differential signal using the proposed method. In this method, IL300 voltage sensor and ACS712 current sensor were used to sense the excited waveforms.

VII. MEASUREMENT

The proposed methods of using existing hardware- DC/DC and AC/DC power electronics, protection circuitry, battery balancing, and separate excitation circuit represent a promising set of results all indicating that it is possible to generate a low-frequency excitation signal to undertake on-line EIS measurement. However, it is not sufficient to merely produce an excitation signal. In order to get useful information out of the system, the following additional processes need to occur;

1) The battery voltage and current need to be accurately measured to enable a mV excitation signal (of similar magnitude to those in Table 1) to be detected. As this work is still at early stages, some authors have used highly accurate scopes [31], [38], [47], [49] whilst others have used current and voltage sensors, battery management system and analogue-to-digital converter [28], [29], [32], [35], [36], [41], [42], [53].
2) Once the measurements have occurred the low-frequency component needs to be extracted using some form of FFT. Although this can be done offline, [35], [42], and [44] report doing this online using a digital signal processing algorithm to calculate and extract the impedance of the battery from the current and voltage measurement. The impedance calculation algorithms used by authors include a digital lock-in amplifier technique and FFT algorithm. These algorithms were reported to be implemented in DSP, Lab-view, or bespoke signal processing hardware by the authors.
3) The voltage and current need to be divided to get the impedance at the harmonic of interest and this data can

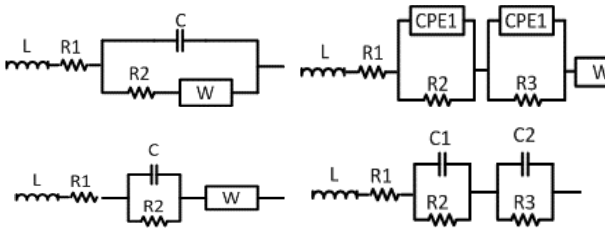

FIGURE 19. common equivalent circuit represented by literature.

be turned into a Nyquist plot. However, it is more useful to take the data and then fit this to an impedance model to allow equivalent circuit parameters to be estimated. Typical models used in literature include the equivalent circuit models in Fig. 19 [28], [32], [40], [42], [49]. In a fitting method, the impedance data of the battery is used as a basis to curve fitting battery model parameters. An equivalent circuit of the battery impedance curve is used to fit the impedance data over the frequency domain. A complex nonlinear least square method can be undertaken to predict the parameter values of the battery equivalent circuit to match the measured impedance data [36], [44].

4) Once an equivalent circuit has been established this can be related back to chemical processes to look for signs of problems or used within a state of charge (SOC) or state of health (SOH) calculation.
5) The battery impedance is known to change with SOC and temperature, so the impedance and subsequent Nyquist plot is not constant but continually changing with time online. Research is needed into how to deal with data under these conditions and is previously only briefly mentioned in [42].

VIII. CONCLUSION

A comparison chart of the online impedance measurement methods is shown in Table 2. This focuses on additional hardware cost, additional ripple to any power electronic inductor resulting in a re-design and other known reported issues.

This paper compared different methods of generating a low-frequency excitation signal and attempted to classify them. In most cases, these methods can be undertaken using hardware found in most battery systems. The operation principle of each technique was explained and some waveforms of the system under operation were shown. In all the proposed methods, the low-frequency component has been detected within the measured battery waveforms from the experimental setup. This indicates the possibility of using these methods to undertake and implement an online EIS measurement. However, there are potential trade-offs, for example, using dc/dc power electronic converter hardware to generate the excitation signal could result in the need for a re-design of the inductor due to increased ripple through it. What is clear is that this area of research is undergoing a rapid change and there is potential to undertake significantly more research in this area looking at different circuit topologies, different control techniques and different methods of collecting, analysing and using the data to provide information.

TABLE 2. EIS comparison.

Method	Added hard-ware	Inductor ripple current	Issues
Separate excitation circuit	y	n	Cost of hardware
Shunting resistor balancing	n	n	Measurement in discharge only and excitation dependent on imbalance
Ladder inductor balancing	n	n	Measurement and excitation dependent on imbalance
Switched capacitor balancing	n	n	Measurement dependent on imbalance
AC/DC power electronics	n	n	Measurement may be in discharge/at fundamental frequency of inverter
Diagnosis mode	n	n	Needs to be taken off-line for batteries
Variable voltage set point	n	y	Increased inductor ripple
Variable duty cycle	n	y	Increased inductor ripple
Variable switching frequency	n	y	Difficult to get level of accuracy required
Variable starting point	n	y	Difficult to get level of accuracy required
Impulse function	n	y	Difficult to control
Protection (ELM)	n	n	Dependent on further manufacturer development

Within the presented work, only a limited amount of research has been done on battery balancing to date as a method of generating EIS excitation signals. There is scope for future work to look at other battery balancing methods to produce a low-frequency excitation signal for impedance measurement. Also, in a switched capacitor balancing circuit, a series resonant inductor may be considered for soft switching. Further work is required to look into the effect of the resonant switched capacitor balancing circuit to produce a perturbation signal. Further improvements to the design of the DC-DC converter is needed such that the switching frequency can be increased to allow operation at higher frequency points which would also allow the system to be applied to different applications such as solar cell monitoring and fuel cell monitoring.

ACKNOWLEDGMENT

Applicable data is available on the Loughborough University data repository.

REFERENCES

[1] X. Hu, C. Zou, C. Zhang, and Y. Li, "Technological developments in batteries: A survey of principal roles, types, and management needs," *IEEE Power Energy Mag.*, vol. 15, no. 5, pp. 20–31, Sep. 2017.
[2] A. Zenati, P. Desprez, H. Razik, and S. Rael, "Impedance measurements combined with the fuzzy logic methodology to assess the SOC and SOH of lithium-ion cells," in *Proc. IEEE Veh. Power Propulsion Conf. (VPPC)*, Sep. 2010, pp. 1–6.

[3] A. Zenati, P. Desprez, and H. Razik, "Estimation of the SOC and the SOH of li-ion batteries, by combining impedance measurements with the fuzzy logic inference," in *Proc. 36th Annu. Conf. IEEE Ind. Electron. Soc. (IECON)*, Nov. 2010, pp. 1773–1778.

[4] L. Ran, W. Junfeng, W. Haiying, and L. Gechen, "Prediction of state of charge of Lithium-ion rechargeable battery with electrochemical impedance spectroscopy theory," in *Proc. 5th IEEE Conf. Ind. Electron. Appl. (ICIEA)*, Jun. 2010, pp. 684–688.

[5] P.-C. Wu, W.-C. Hsu, and J.-F. Chen, "Detection on SOC of VRLA battery with EIS," in *Proc. 1st Int. Future Energy Electron. Conf. (IFEEC)*, Nov. 2013, pp. 897–902.

[6] J. Chiasson and B. Vairamohan, "Estimating the state of charge of a battery," *IEEE Trans. Control Syst. Technol.*, vol. 13, no. 3, pp. 465–470, May 2005.

[7] F. Xuyun and S. Zechang, "A battery model including hysteresis for State-of-Charge estimation in Ni-MH battery," in *Proc. IEEE Veh. Power Propuls. Conf. (VPPC)*, Sep. 2008, pp. 1–5.

[8] J. P. Christophersen, J. Morrison, W. Morrison, and C. Motloch, "Rapid impedance spectrum measurements for state-of-health assessment of energy storage devices," *SAE Int. J. Passenger Cars-Electron. Electr. Syst.*, vol. 5, no. 1, p. 01-2012-0657, 2012.

[9] S. J. Lee, J. H. Kim, J. M. Lee, and B. H. Cho, "The state and parameter estimation of an Li-Ion battery using a new OCV-SOC concept," in *Proc. Power Electron. Specialists Conf. (PESC)*, 2007, pp. 2799–2803.

[10] J. P. Christophersen, J. L. Morrison, and W. H. Morrison, "Acquiring impedance spectra from diode-coupled primary batteries to determine health and state of charge," in *Proc. Aerosp. Conf.*, 2013, pp. 1–10.

[11] M. Hejabi, A. Oweisi, and N. Gharib, "Modeling of kinetic behavior of the lead dioxide electrode in a lead-acid battery by means of electrochemical impedance spectroscopy," *J. Power Sources*, vol. 158, no. 2, pp. 944–948, 2006.

[12] M. Galeotti, C. Giammanco, L. Cina, S. Cordiner, and A. Di Carlo, "Diagnostic methods for the evaluation of the state of health (SOH) of NiMH batteries through electrochemical impedance spectroscopy," in *Proc. IEEE 23rd Int. Symp. Ind. Electron. (ISIE)*, Jun. 2014, pp. 1641–1646.

[13] C. Zou, X. Hu, S. Dey, L. Zhang, and X. Tang, "Nonlinear fractional-order estimator with guaranteed robustness and stability for lithium-ion batteries," *IEEE Trans. Ind. Electron.*, to be published.

[14] M. Swierczynski, D. I. Stroe, A.-I. Stan, R. Teodorescu, and D. U. Sauer, "Selection and performance-degradation modeling of $LiMO_2/Li_4Ti_5O_{12}$ and LiFePO 4/C battery cells as suitable energy storage systems for grid integration with wind power plants: An example for the primary frequency regulation service," *IEEE Trans. Sustain. Energy*, vol. 5, no. 1, pp. 90–101, Jan. 2014.

[15] J. Li *et al.*, "Calcium metaborate as a cathode additive to improve the high-temperature properties of nickel hydroxide electrodes for nickel-metal hydride batteries," *J. Power Sources*, vol. 263, pp. 110–117, Oct. 2014.

[16] F. Kramm, "Influence of temperature and charging voltage on the endurance of VRLA-batteries," in *Proc. Power Energy Syst. Converging Markets*, 1997, pp. 25–28.

[17] M. Umeda, K. Dokko, Y. Fujita, M. Mohamedi, I. Uchida, and J. R. Selman, "Electrochemical impedance study of Li-Ion insertion into mesocarbon microbead single particle electrode: Part I. Graphitized carbon," *Electrochim. Acta*, vol. 47, no. 6, pp. 885–890, 2001.

[18] A. Li *et al.*, "Electrochemical behavior and application of lead-lanthanum alloys for positive grids of lead-acid batteries," *J. Power Sources*, vol. 189, no. 2, pp. 1204–1211, 2009.

[19] B. Yang, Z. Yang, Z. Peng, and Q. Liao, "Effect of silver additive on the electrochemical performance of ZnAl-layered double hydroxide as anode material for nickel-zinc rechargeable batteries," *Electrochim. Acta*, vol. 132, pp. 83–90, Jun. 2014.

[20] B.-L. He, B. Dong, and H.-L. Li, "Preparation and electrochemical properties of Ag-modified TiO2 nanotube anode material for lithium-ion battery," *Electrochem. commun.*, vol. 9, no. 3, pp. 425–430, 2007.

[21] W. Liu, C. Delacourt, C. Forgez, and S. Pelissier, "Study of graphite/NCA Li-ion cell degradation during accelerated aging tests—Data analysis of the SimStock project," in *Proc. IEEE Veh. Power Propuls. Conf. (VPPC)*, Sep. 2011, pp. 1–6.

[22] J. P. Christophersen, D. F. Glenn, C. G. Motloch, R. B. Wright, C. D. Ho, and V. S. Battaglia, "Electrochemical impedance spectroscopy testing on the Advanced Technology Development Program lithium-ion cells," in *Proc. IEEE 56th Veh. Technol. Conf. (VTC-Fall)*, vol. 3. Sep. 2002, pp. 1851–1855.

[23] L. Lam and P. Bauer, "Practical capacity fading model for Li-ion battery cells in electric vehicles," *IEEE Trans. Power Electron.*, vol. 28, no. 12, pp. 5910–5918, Dec. 2013.

[24] L. F. Q. P. Marchesi, F. R. Simões, L. A. Pocrifka, and E. C. Pereira, "Investigation of polypyrrole degradation using electrochemical impedance spectroscopy," *J. Phys. Chem. B*, vol. 115, no. 31, pp. 9570–9575, 2011.

[25] N. D. Cogger and N. J. Evans. (1999). *An Introduction to Electrochemical Impedance Measurement*. [Online]. Available: http://www.korozja.pl/html/eis/technote06.pdf

[26] B. Hong *et al.*, "Characterization of nano-lead-doped active carbon and its application in lead-acid battery," *J. Power Sources*, vol. 270, pp. 332–341, Dec. 2014.

[27] P. Neti and S. Grubic, "Online broadband insulation spectroscopy of induction machines using signal injection," in *Proc. IEEE Energy Convers. Congr. Expo. (ECCE)*, 2014, pp. 630–637.

[28] L. Zhao, Q. Fu, and Z. Liu, "An electrochemical impedance spectroscopy measurement system for electric vehicle batteries," in *Proc. 35th Chin. Control Conf. (CCC)*, 2016, pp. 5050–5055.

[29] X. Wang, X. Wei, H. Dai, and Q. Wu, "State estimation of lithium ion battery based on electrochemical impedance spectroscopy with on-board impedance measurement system," in *Proc. IEEE Veh. Power Propulsion Conf. (VPPC)*, Oct. 2015, pp. 1–5.

[30] U. Tröltzsch and O. Kanoun, "Miniaturized Impedance Measurement System for Battery Diagnosis," in *Proc. SENSOR*, 2009, pp. 251–256.

[31] L.-R. Chen, S.-L. Wu, D.-T. Shieh, and T.-R. Chen, "Sinusoidal-ripple-current charging strategy and optimal charging frequency study for li-ion batteries," *IEEE Trans. Ind. Electron.*, vol. 60, no. 1, pp. 88–97, Jan. 2013.

[32] S.-Y. Cho, I.-O. Lee, J.-I. Baek, and G.-W. Moon, "Battery impedance analysis considering DC component in sinusoidal ripple-current charging," *IEEE Trans. Ind. Electron.*, vol. 63, no. 3, pp. 1561–1573, Mar. 2016.

[33] A. J. Fairweather, M. P. Foster, and D. A. Stone, "VRLA battery parameter identification using pseudo random binary sequences (PRBS)," in *Proc. 5th IET Int. Conf. Power Electron., Mach. Drives (PEMD)*, 2010, pp. 1–6.

[34] M. Ranieri, D. Alberto, H. Piret, and V. Cattin, "Electronic module for the thermal monitoring of a Li-ion battery cell through the electrochemical impedance estimation," in *Proc. 22nd Int. Workshop Thermal Invest. ICs Syst. (THERMINIC)*, 2016, pp. 294–297.

[35] R. Koch, C. Riebel, and A. Jossen, "On-line electrochemical impedance spectroscopy implementation for telecommunication power supplies," in *Proc. IEEE Int. Telecommun. Energy Conf. (INTELEC)*, Oct. 2015, pp. 1–6.

[36] E. Din, C. Schaef, K. Moffat, and J. Stauth, "A scalable active battery management system with embedded real-time electrochemical impedance spectroscopy," *IEEE Trans. Power Electron.*, vol. 32, no. 7, pp. 5688–5698, Jul. 2017.

[37] E. Din, C. Schaef, K. Moffat, and J. T. Stauth, "Online spectroscopic diagnostics implemented in an efficient battery management system," in *Proc. IEEE 16th Workshop Control Modeling Power Electron.*, Jun. 2015, pp. 1–7.

[38] M. A. Varnosfaderani, *Investigation of Different Methods of Online Impedance Spectroscopy of Batteries*. Birmingham, U.K.: Aston Univ., 2017.

[39] A. Ahmed, *Series Resonant Switched Capacitor Converter for Electric Vehicle Lithium-Ion Battery Cell Voltage Equalization*. Mequon, WI, USA: Concordia Univ., 2012.

[40] R. Koch, R. Kuhn, I. Zilberman, and A. Jossen, "Electrochemical impedance spectroscopy for online battery monitoring—Power electronics control," in *Proc. 16th Eur. Conf. Power Electron. Appl. (EPE-ECCE Europe)*, 2014, pp. 1–10.

[41] R. Koch and A. Jossen, "Impedance spectroscopy for battery monitoring with switched mode," in *Proc. PEMC*, 2014, pp. 496–501.

[42] D. A. Howey, P. D. Mitcheson, V. Yufit, G. J. Offer, and N. P. Brandon, "Online Measurement of Battery Impedance Using Motor Controller Excitation," *IEEE Trans. Veh. Technol.*, vol. 63, no. 6, pp. 2557–2566, Jun. 2014.

[43] N. Katayama and S. Kogoshi, "Real-time electrochemical impedance diagnosis for fuel cells using a DC-DC converter," *IEEE Trans. Energy Convers.*, vol. 30, no. 2, pp. 707–713, Jun. 2015.

[44] T.-T. Nguyen, V.-L. Tran, and W. Choi, "Development of the intelligent charger with battery State-Of-Health estimation using online impedance spectroscopy," in *Proc. IEEE 23rd Int. Symp. Ind. Electron. (ISIE)*, Jun. 2014, pp. 454–458.

[45] V.-T. Doan, V.-B. Vu, H.-N. Vu, D.-H. Tran, and W. Choi, "Intelligent charger with online battery diagnosis function," in *Proc. 9th Int. Conf. Power Electron. ECCE Asia (ICPE-ECCE Asia)*, 2015, pp. 1644–1649.
[46] J. A. A. Qahouq, "Online battery impedance spectrum measurement method," in *Proc. IEEE Appl. Power Electron. Conf. Expo. (APEC)*, Mar. 2016, pp. 3611–3615.
[47] J. A. A. Qahouq and Z. Xia, "Single-perturbation-cycle online battery impedance spectrum measurement method with closed-loop control of power converter," *IEEE Trans. Ind. Electron.*, vol. 64, no. 9, pp. 7019–7029, Sep. 2017.
[48] A. Densmore and M. Hanif, "Determining battery SoC using electrochemical impedance spectroscopy and the extreme learning machine," in *Proc. IEEE 2nd Int. Future Energy Electron. Conf.*, Nov. 2015, pp. 1–7.
[49] M. A. Varnosfaderani and D. Strickland, "Online impedance spectroscopy estimation of a battery," in *Proc. 18th Eur. Conf. Power Electron. Appl. (EPEECCE Europe)*, 2016, pp. 1–10.
[50] *Eaton EMR4-R Earth Leakage Monitor*. [Online]. Available: http://www.moeller.net/en/products_solutions/motor_applications/control/measuring_relay/earth_leakage_monitor.jsp
[51] *Thiim Earth Leakage Monitor*. [Online]. Available: http://thiim.com/datasheets/ddea.pdf
[52] M. A. Varnosfaderani and D. Strickland, "Online impedance spectroscopy estimation of a DC-DC converter connected battery using an earth leakage monitoring circuit," in *Proc. 19th Eur. Conf. Power Electron. Appl. (EPE ECCE Europe)*, Sep. 2017, pp. P.1–P.10.
[53] D. Depernet, O. Ba, and A. Berthon, "Online impedance spectroscopy of lead acid batteries for storage management of a standalone power plant," *J. Power Sour.*, vol. 219, pp. 65–74, Dec. 2012.

MINA ABEDI VARNOSFADERANI received the M.Eng. degree in electrical and electronics engineering from the University of Birmingham and the Ph.D. degree in electrical engineering from Aston University, Birmingham, U.K. She is currently with Loughborough University as a Research Associate. Her research interests include hybrid batteries and power-sharing systems.

DANI STRICKLAND received the degree from Heriot Watt University and the Ph.D. degree in electrical engineering from Cambridge University, U.K. She was with Eon, Sheffield University, Rolls Royce Fuel Cells PLC, and Aston University. She is currently with Loughborough University as a Senior Lecturer. Her main research interests include the application of power electronics to power systems.